JOURNAL OF COMPUTATIONAL PHYSICS 24, 372–397 (1977)

# Solution of the Multidimensional Compressible Navier–Stokes Equations by a Generalized Implicit Method

W. R. BRILEY* AND H. MCDONALD*

*United Technologies Research Center, East Hartford, Connecticut 06108*

Received June 21, 1976; revised October 7, 1976

In an effort to exploit the favorable stability properties of implicit methods and thereby increase computational efficiency by taking large time steps, an implicit finite-difference method for the multidimensional Navier–Stokes equations is presented. The method consists of a generalized implicit scheme which has been linearized by Taylor expansion about the solution at the known time level to produce a set of coupled linear difference equations which are valid for a given time step. To solve these difference equations, the Douglas–Gunn procedure for generating alternating-direction implicit (ADI) schemes as perturbations of fundamental implicit difference schemes is employed. The resulting sequence of narrow block-banded systems can be solved efficiently by standard block-elimination methods. The method is a one-step method, as opposed to a predictor-corrector method, and requires no iteration to compute the solution for a single time step. Test calculations are presented for a three-dimensional application to subsonic flow in a straight duct with rectangular cross section. Stability is demonstrated for time steps which are orders of magnitude larger than the maximum allowable time step for conditionally stable methods as determined by the well-known CFL condition. The computational effort per time step is discussed and is very approximately only twice that of most explicit methods. The accuracy of computed solutions is examined by mesh refinement and comparison with other analytical and experimental results.

## INTRODUCTION

One of the major obstacles to the routine numerical solution of the multidimensional compressible Navier–Stokes equations is the large amount of computer time generally required, and consequently, efficient computational methods are highly desirable in this instance. Most previous methods for solving the compressible Navier–Stokes equations have been based on explicit difference schemes for the unsteady form of the governing equations and are subject to one or more stability restrictions on the size of the time step relative to the spatial mesh size. These stability limits usually correspond to the well-known Courant–Friedrichs–Lewy (CFL) condition and, in some schemes, to an additional stability condition arising from viscous terms. In one dimension, the CFL condition is $\Delta t \leqslant \Delta x/(|u| + c)$, and the viscous stability condition is $\Delta t \leqslant (\Delta x)^2/2\nu$, where $\Delta t$ is the time step, $\Delta x$ is the mesh size, $u$ is velocity,

* Present address: Scientific Research Associates, Inc., P. O. Box 498, Glastonbury, Connecticut 06033.





ISSN 0021-9991

$c$ is the speed of sound, and $\nu$ is kinematic viscosity. These stability restrictions can lower computational efficiency by imposing a smaller time step than would otherwise be desirable. Thus, a key disadvantage of conditionally stable methods is that the maximum time step is fixed by the spatial mesh size rather than the physical time dependence or the desired temporal accuracy. In contrast to most explicit methods, implicit methods tend to be stable for large time steps and hence offer the prospect of substantial increases in computational efficiency, provided of course that large time steps are acceptable for the physical problem of interest and that the computational effort per time step is competitive with that of explicit methods. In an effort to exploit these potentially favorable stability properties, an efficient implicit method based on alternating-direction differencing techniques was developed and is presented herein.

## The Present Method

The present method can be briefly outlined as follows. The governing equations are replaced by an implicit time difference approximation, optionally a backward difference or Crank–Nicolson scheme. Terms involving nonlinearities at the implicit time level are linearized by Taylor expansion about the solution at the known time level, and spatial difference approximations are introduced. The result is a system of multidimensional coupled (but linear) difference equations for the dependent variables at the unknown or implicit time level. To solve these difference equations, the Douglas–Gunn [1] procedure for generating alternating-direction implicit (ADI) schemes as perturbations of fundamental implicit difference schemes is introduced. This technique leads to systems of coupled linear difference equations having narrow block-banded matrix structures which can be solved efficiently by standard block-elimination methods.

The method centers around the use of a formal linearization technique adapted for the integration of initial-value problems. The linearization technique, which of necessity requires an implicit solution procedure, permits the solution of coupled nonlinear equations in one space dimension (to the requisite degree of accuracy) by a one-step noniterative scheme. Since no iteration is required to compute the solution for a single time step, and since only moderate effort is required for solution of the implicit difference equations, the method is computationally efficient; this efficiency is retained for multidimensional problems by using ADI techniques. The method is also economical in terms of storage, in its present form requiring only two time levels of storage for each dependent variable. Furthermore, the ADI technique reduces multidimensional problems to sequences of calculations which are one-dimensional in the sense that easily-solved narrow block-banded matrices associated with one-dimensional rows of grid points are produced. Consequently, only these one-dimensional problems require rapid-access storage at any given stage of the solution procedure, and the remaining flow variables can be saved on auxiliary storage devices if desired.

## APPLICABILITY

Although present attention is focused on the compressible Navier–Stokes equations, the numerical method employed is quite general and is formally derived for systems of governing equations which have the form

$$\partial H(\phi)\,\partial t = \mathscr{D}(\phi) + S(\phi) \tag{1}$$

where $\phi$ is a column vector containing $l$ dependent variables, $H$ and $S$ are column vector functions of $\phi$, and $\mathscr{D}$ is a column vector whose elements are spatial differential operators which may be multidimensional. The generality of (1) allows the method to be developed concisely and permits various extensions and modifications (e.g., noncartesian coordinate systems, turbulence models) to be made more or less routinely. It should be emphasized however, that the Jacobian $\partial H/\partial\phi$ must usually be nonsingular if the ADI techniques as applied to (1) are to be valid. A necessary condition is that each dependent variable appear in one or more of the governing equations as a time derivative. An exception would occur if for instance, a variable having no time derivative also appeared in only one equation, so that this equation could be decoupled from the remaining equations and solved a posteriori by an alternate method. As a consequence, the present method is not directly applicable to the incompressible Navier–Stokes equations except in one dimension, where ADI techniques are unnecessary. For example, the velocity–pressure form of the incompressible equations has no time derivative of stream function. For computing steady solutions, however, the addition of suitable "artificial" time derivatives to the incompressible equations, as was done in Chorin's [2] artificial compressibility method, would permit the application of the present method. Alternatively, a low Mach number solution of the compressible equations can be computed.

For low Mach number flows, the CFL condition eventually becomes restrictive regardless of mesh spacing, and thus stable implicit methods are well suited for problems in the low Mach number regime. For all Mach numbers, both the CFL and viscous stability conditions eventually become restrictive for sufficiently small mesh spacing. Implicit methods thus become increasingly attractive when high spatial resolution is necessary and when locally refined meshes are used. This latter situation is common when more than one length scale is present, as is the case for flows which are largely inviscid but have thin boundary layers requiring a locally refined mesh. Similar statements hold for (time-averaged) turbulent flows with viscous sublayers.

## GOVERNING EQUATIONS

The numerical method is presented for flow in three space dimensions; two-dimensional problems can be treated as a special case. For simplicity, it is assumed that the fluid is a perfect gas with zero bulk viscosity coefficient and constant molecular viscosity, thermal conductivity, and specific heat. The governing equations are

nondimensionalized by normalizing dimensional variables with the following reference quantities: distance, $L_r$; velocity, $U_r$; density, $\rho_r$, temperature; $T_r$; time, $L_r/U_r$; enthalpy $U_r^2$; and pressure, $\rho_r U_r^2/g$, where $g$ is the gravitational constant. This normalization leads to the nondimensional parameters: Mach number, $M$; Reynolds number, Re; Prandtl number, Pr; and specific heat ratio, $\gamma$. These parameters are defined by

$$M = U_r/c, \quad \mathrm{Re} = \rho_r U_r L_r/\mu, \quad \mathrm{Pr} = c_p\mu/k, \quad \gamma = c_p/c_v \qquad \text{(2a)–(2d)}$$

where $\mu$ is the molecular viscosity, $k$ is thermal conductivity, and $c_p$ and $c_v$ are the specific heats at constant pressure and volume. The reference speed of sound, $c$, is defined by $c^2 = \gamma g R T_r$, where $R$ is the gas constant.

With the exception of the energy equation, the equations are written in the so-called conservation form. The foregoing assumptions are convenient but not essential; the treatment of alternate forms of the equations, arbitrary equation of state, and variable fluid properties is relatively straightforward. With the stated assumptions, the Navier–Stokes equations can be written for Cartesian coordinates $(x, y, z)$ as follows: The continuity equation is

$$\partial\rho/\partial t = \partial(-\rho u)/\partial x + \partial(-\rho v)/\partial y + \partial(-\rho w)/\partial z. \qquad \text{(3a)}$$

The $j$th momentum equation is given by

$$\partial(\rho U_j)/\partial t = \partial(-\rho u U_j)/\partial x + \partial(-\rho v U_j)/\partial y + \partial(-\rho w U_j)/\partial z - \partial p/\partial X_j + F_j\,. \qquad \text{(3b)}$$

The energy equation is

$$\frac{\partial \rho T}{\partial t} = \frac{\partial}{\partial x}\left(-\rho u T + \frac{\gamma}{\mathrm{Re\,Pr}}\frac{\partial T}{\partial x}\right) + \frac{\partial}{\partial y}\left(-\rho v T + \frac{\gamma}{\mathrm{Re\,Pr}}\frac{\partial T}{\partial y}\right) + \frac{\partial}{\partial z}\left(-\rho w T + \frac{\gamma}{\mathrm{Re\,Pr}}\frac{\partial T}{\partial z}\right) + \gamma(\gamma-1)\,M^2\left[\frac{1}{\mathrm{Re}}\Phi - p(\nabla\cdot U)\right]. \qquad \text{(3c)}$$

In (3), $U$ is the velocity vector with components $U_j = u, v, w$; $X$ is the position vector with components $X_j = x, y, z$; $\rho$ is density; $T$ is temperature; $p$ is pressure; $t$ is time, and $\Delta$ is the gradient operator. The force $F$ due to viscous stress has components given by

$$F_j = (1/\mathrm{Re})[\nabla^2 U_j + \tfrac{1}{3}\partial(\nabla\cdot U)/\partial X_j]. \qquad (4)$$

The dissipation function, $\Phi$, is given by

$$\Phi = 2\left[\left(\frac{\partial u}{\partial x}\right)^2 + \left(\frac{\partial v}{\partial y}\right)^2 + \left(\frac{\partial w}{\partial z}\right)^2\right] + \left(\frac{\partial u}{\partial y} + \frac{\partial v}{\partial x}\right)^2 + \left(\frac{\partial v}{\partial z} + \frac{\partial w}{\partial y}\right)^2 + \left(\frac{\partial u}{\partial z} + \frac{\partial w}{\partial x}\right)^2 - \frac{2}{3}(\nabla\cdot U)^2. \qquad (5)$$

The pressure can be eliminated as a dependent variable by means of the equation of state for a perfect gas,

$$p = \rho T/\gamma M^2. \tag{6}$$

The continuity, momentum, and energy equations thus constitute a system of five equations in the dependent variables $\rho$, $u$, $v$, $w$, and $T$. The definition of total enthalpy $E$ is

$$E = T/(\gamma - 1)\, M^2 + q^2/2 \tag{7}$$

where $q^2 = u^2 + v^2 + w^2$. In numerous problems of interest, it can be assumed that the total enthalpy is a constant $E_0$ provided there is no heat addition. This assumption is reasonable for inviscid flow regions with or without shocks and for boundary layers on adiabatic walls provided the Prandtl number is unity. In this circumstance, (6) and (7) can be combined to produce an adiabatic equation of state,

$$p = \rho(E_0 - q^2/2)(\gamma - 1)/\gamma. \tag{8}$$

If pressure is eliminated in the momentum equations by means of (8), then a solution of energy equation (3c) is unnecessary, and a significant reduction in computational effort is effected. The temperature field is then determined a posteriori from (7). This simplification, although convenient and available as an option, was not used for any of the calculations presented here for laminar flow.

## Numerical Method

### *Previous Work*

Although several methods based on implicit schemes have been developed for incompressible flows (e.g., [3], [4]), most previous methods for the compressible Navier–Stokes equations have employed explicit schemes. Nevertheless, a semi-implicit method has been developed by Harlow and Amsden [5] for use over the entire spectrum of Mach numbers from incompressible to hypersonic. However, the Harlow–Amsden method treats viscous terms explicitly and, unlike alternating-direction methods, requires the solution of multidimensional implicit difference equations, which tends to be time consuming. In an independent investigation, Baum and Ndefo [6] developed a two-dimensional implicit method which is patterned after the original Peaceman–Rachford [7] ADI technique. Perhaps the most significant difference between the Baum–Ndefo and present methods is that the Baum–Ndefo method employs iterative techniques, solving nonlinear difference equations as a sequence of linear equation, whereas in the present method, the difference equations are linearized about the solution at the previous time step and solved without iteration. In principle, the solution of nonlinear difference equations is of course attractive, as this removes any limitations which might arise from the linearization process.

It is, however, a time-consuming process to solve the nonlinear difference equations, and as far as temporal accuracy is concerned, the additional computational effort required by the solution of nonlinear difference equations might be as well spent by reducing the time step and proceeding with a satisfactory linearization [8]. On the other hand, if a steady solution is the only objective, then temporal accuracy is of little concern, and a stable method requiring minimal computational effort per time step (the present objective) is attractive. The topic of nonlinear truncation errors is discussed further by McDonald and Briley [8].

The present numerical method was developed for the Navier–Stokes equations by Briley and McDonald [9] and for steady supersonic flows by McDonald and Briley [8]. Here the method is formalized for mixed parabolic–hyperbolic systems having the form of (1), and is applied to the Navier–Stokes equations. Recently, Beam and Warming [10] have followed a similar approach and have specialized this same linearization procedure to equations in conservation-law form, with emphasis on the inviscid Euler equations. Beam and Warming employed a locally one-dimensional (LOD) scheme and compact spatial differencing techniques analogous to those discussed by Mitchell [11, p. 51, 61], but in the special circumstances of the Euler equations.

## Linearization Technique

### *Background*

A number of techniques have been used for implicit solution of the following first-order nonlinear scalar equation in one dependent variable $\phi(x, t)$

$$\partial\phi/\partial t = F(\phi)\, \partial G(\phi)/\partial x. \tag{9}$$

Special cases of (9) include the conservation form if $F(\phi) = 1$, and quasi-linear form if $G(\phi) = \phi$. Previous implicit methods for (9) which employ nonlinear difference equations and also methods based on two-step predictor-corrector schemes are discussed by Ames [12, p. 82] and von Rosenberg [13, p. 56]. One such method is to difference nonlinear terms directly at the implicit time level to obtain nonlinear implicit difference equations; these are then solved iteratively by a procedure such as Newton's method. Although otherwise attractive, there may be difficulty with convergence in the iterative solution of the nonlinear difference equations, and some efficiency is sacrificed by the need for iteration. An implicit predictor-corrector technique has been devised by Douglas and Jones [14] which is applicable to the quasi-linear case ($G = \phi$) of (9). The first step of their procedure is to linearize the equation by evaluating the nonlinear coefficient as $F(\phi^n)$ and to predict values of $\phi^{n+1/2}$ using either the backward difference or the Crank–Nicolson scheme. Values for $\phi^{n+1}$ are then computed in a similar manner using $F(\phi^{n+1/2})$ and the Crank–Nicolson scheme. Gourlay and Morris [15] have also proposed implicit predictor-

corrector techniques which can be applied to (9). In the conservative case ($F = 1$), their technique is to define $\hat{G}(\phi)$ by the relation $G(\phi) = \phi\hat{G}(\phi)$ when such a definition exists, and to evaluate $\hat{G}(\phi^{n+1})$ using values for $\phi^{n+1}$ computed by an explicit predictor scheme. With $\hat{G}$ thereby known at the implicit time level, the equation can be treated as linear, and corrected values of $\phi^{n+1}$ are computed by the Crank–Nicolson scheme.

A technique is described here for deriving linear implicit difference approximations for nonlinear differential equations. The technique is based on an expansion of nonlinear implicit terms about the solution at the known time level, $t^n$, and leads to a one-step, two-level scheme which, being linear in unknown (implicit) quantities, can be solved efficiently without iteration. This idea was applied by Richtmyer and Morton [16, p. 203] to a scalar nonlinear diffusion equation. Here, the technique is developed for problems governed by $l$ nonlinear equations in $l$ dependent variables which are functions of time and space coordinates. Attention is restricted to nonlinear systems having the form of (1).

The solution domain is discretized by grid points having equal spacings, $\Delta x$, $\Delta y$, and $\Delta z$, in the $x$, $y$, and $z$ directions, respectively, and an arbitrary time step, $\Delta t$. Provisions for nonuniform grid spacing will be introduced subsequently. The subscripts $i, j, k$, and superscript $n$ are grid point indices associated with $x$, $y$, $z$, and $t$, respectively, and thus $\phi^n_{i,j,k}$ denotes $\phi(x_i, y_j, z_k, t^n)$. It is assumed that the solution is known at the $n$ level, $t^n$, and is desired at the $(n + 1)$ level, $t^{n+1}$. At the risk of an occasional ambiguity, one or more of the subscripts is frequently omitted, so that $\phi^n$ is equivalent to $\phi^n_{i,j,k}$.

*Linearized Difference Scheme*

The linearization technique is a simple one which can be illustrated by application to the one-dimensional continuity equation. Using backward time differences, the continuity equation is expanded as

$$\frac{\rho^{n+1} - \rho^n}{\Delta t} = -\frac{\partial}{\partial x}(\rho u)^{n+1}$$

$$= -\frac{\partial}{\partial x}\left[(\rho u)^n + \left(\frac{\partial \rho u}{\partial \rho}\frac{\partial \rho}{\partial t} + \frac{\partial \rho u}{\partial u}\frac{\partial u}{\partial t}\right)^n \Delta t + O(\Delta t)^2\right] \tag{10}$$

(10) is time differenced to obtain

$$\frac{\rho^{n+1} - \rho^n}{\Delta t} = -\frac{\partial}{\partial x}\left[\rho^n u^n + u^n\left(\frac{\rho^{n+1} - \rho^n}{\Delta t}\right)\Delta t + \rho^n\left(\frac{u^{n+1} - u^n}{\Delta t}\right)\Delta t\right]$$

$$= -\frac{\partial}{\partial x}(\rho^{n+1}u^n + \rho^n u^{n+1} - \rho^n u^n) \tag{11}$$

which is linear and couples $\rho^{n+1}$ and $u^{n+1}$. Having given a simple illustration of the technique, attention is now devoted to systems of equations having the form of (1).

The linearized difference approximation is derived from the following implicit time-difference replacement

$$(H^{n+1} - H^n)/\Delta t = \beta[\mathscr{D}(\phi^{n+1}) + S^{n+1}] + (1 - \beta)[\mathscr{D}(\phi^n) + S^n] \tag{12}$$

where, for example, $H^{n+1} \equiv H(\phi^{n+1})$. The form of $\mathscr{D}$ and the spatial differencing are as yet unspecified. Here, a parameter $\beta$ ($0 \leqslant \beta \leqslant 1$) has been introduced so as to permit a variable centering of the scheme in time. Equation (12) produces a backward difference formulation for $\beta = 1$ and a Crank–Nicolson formulation for $\beta = \frac{1}{2}$. Unconditional stability is anticipated for $\beta > \frac{1}{2}$.

The linearization is performed by a two-step process of expansion about the known time level $t^n$ and subsequent approximation of the quantity $(\partial\phi/\partial t)^n \Delta t$, which arises from chain rule differentiation, by $(\phi^{n+1} - \phi^n)$. The result is

$$H^{n+1} = H^n + (\partial H/\partial\phi)^n(\phi^{n+1} - \phi^n) + O(\Delta t)^2, \tag{13a}$$

$$S^{n+1} = S^n + (\partial S/\partial\phi)^n(\phi^{n+1} - \phi^n) + O(\Delta t)^2, \tag{13b}$$

$$\mathscr{D}(\phi^{n+1}) = \mathscr{D}(\phi^n) + (\partial\mathscr{D}/\partial\phi)^n(\phi^{n+1} - \phi^n) + O(\Delta t)^2. \tag{13c}$$

The matrices $\partial H/\partial\phi$ and $\partial S/\partial\phi$ are standard Jacobians whose elements are defined, for example, by $(\partial H/\partial\phi)_{qr} \equiv \partial H_q/\partial\phi_r$. The operator elements of the matrix $\partial\mathscr{D}/\partial\phi$ are similarly ordered, i.e., $(\partial\mathscr{D}/\partial\phi)_{qr} \equiv \partial\mathscr{D}_q/\partial\phi_r$; however, the intended meaning of the operator elements requires some clarification. For the $q$th row, the operation $(\partial\mathscr{D}_q/\partial\phi)^n(\phi^{n+1} - \phi^n)$ is understood to mean that $\{\partial/\partial t\, \mathscr{D}_q[\phi(x, y, z, t)]\}^n \Delta t$ is computed and that all occurrences of $(\partial\phi_r/\partial t)^n$ arising from chain rule differentiation are replaced by $(\phi_r^{n+1} - \phi_r^n)/\Delta t$.

After linearization as in (13), (12) becomes the linear implicit time-differenced scheme

$$(\partial H^n/\partial\phi)(\phi^{n+1} - \phi^n)/\Delta t = \mathscr{D}(\phi^n) + S^n + \beta(\partial\mathscr{D}/\partial\phi + \partial S^n/\partial\phi)(\phi^{n+1} - \phi^n). \tag{14}$$

Although $H^{n+1}$ is linearized to second order in (13a), the division by $\Delta t$ in (12) introduces an error term of order $\Delta t$. A technique for maintaining formal second-order accuracy in the presence of nonlinear time derivatives is discussed by McDonald and Briley [8], however a three-level scheme results. Second-order temporal accuracy can also be obtained (for $\beta = \frac{1}{2}$) by a change in dependent variable to $\hat{\phi} \equiv H(\phi)$, provided this is convenient, since the nonlinear time derivative is then eliminated. The temporal accuracy is independent of the spatial accuracy.

On examination, it can be seen that (14) is linear in the quantity $(\phi^{n+1} - \phi^n)$ and that all other quantities are either known or evaluated at the $n$ level. Computationally, it is convenient to solve (14) for $(\phi^{n+1} - \phi^n)$ rather than $\phi^{n+1}$. This both simplifies (14) and reduces roundoff errors, since it is presumably better to compute a small $O(\Delta t)$

change in an $O(1)$ quantity than the quantity itself. To simplify the notation, a new dependent variable $\psi$ defined by

$$\psi \equiv \phi - \phi^n \tag{15}$$

is introduced, and thus $\psi^{n+1} = \phi^{n+1} - \phi^n$, and $\psi^n = 0$. It is also convenient to rewrite (14) in the simplified form

$$(A + \Delta t\, \mathscr{L})\, \psi^{n+1} = \Delta t\, [\mathscr{D}(\phi^n) + S^n] \tag{16a}$$

where the following symbols have been introduced to simplify the notation

$$A \equiv \partial H^n/\partial\phi - \beta\, \Delta t(\partial S^n/\partial\phi), \tag{16b}$$

$$\mathscr{L} \equiv -\beta(\partial\mathscr{D}/\partial\phi). \tag{16c}$$

It is noted that $\mathscr{L}(\psi)$ is a linear transformation and thus $\mathscr{L}(0) = 0$. Furthermore, if $\mathscr{D}(\phi)$ is linear, then $\mathscr{L}(\psi) = -\beta\mathscr{D}(\psi)$.

Spatial differencing of (16a) is accomplished simply by replacing derivative operators such as $\partial/\partial x$, $\partial^2/\partial x^2$ by corresponding finite-difference operators, $D_x$, $D_x{}^2$. Henceforth, it is assumed that $\mathscr{D}$ and $\mathscr{L}$ have been discretized in this manner, unless otherwise noted.

*Discussion*

Before proceeding, some general observations seem appropriate. The foregoing linearization technique assumes only that functions are Taylor expandable, an assumption already inherent in the use of a finite-difference method. The governing equations and boundary conditions are addressed directly as a system of coupled nonlinear equations which collectively determine the solution. The approach thus seems more natural than that of making ad hoc linearization and decoupling approximations, as is often done in applying implicit schemes to coupled and/or nonlinear partial differential equations. With the present approach, it is not necessary to associate each governing equation and boundary condition with a particular dependent variable (e.g., to assume $u$ is governed by the $x$ momentum equation, $\rho$ by continuity, etc.) and then to identify various "nonlinear coefficients" and "coupling terms" which must then be treated by lagging, predictor-corrector techniques, or iteration. The Taylor expansion procedure is analogous to that used in the generalized Newton–Raphson or quasi-linearization methods for *iterative* solution of nonlinear systems by expansion about a known *current guess* at the solution (e.g., [17]). However, the concept of expanding about the previous time level has apparently not been employed to produce a noniterative implicit time-dependent scheme for coupled equations, wherein nonlinear terms are approximated to a level of accuracy commensurate with that of the time differencing. The linearization technique also permits the

implicit treatment of coupled nonlinear boundary conditions, such as stagnation pressure and enthalpy at subsonic inlet boundaries, and in practice, this latter feature was found to be crucial to the stability of the overall method.

## Application of Alternating-Direction Techniques

Solution of (16a) is accomplished by application of an alternating-direction implicit (ADI) technique for parabolic–hyperbolic equations. The original ADI method was introduced by Peaceman and Rachford [7] and Douglas [18]; however, the alternating-direction concept has since been expanded and generalized. A discussion of various alternating-direction techniques is given by Mitchell [11] and Yanenko [19]. The present technique is simply an application of the very general procedure developed by Douglas and Gunn [1] for generating ADI schemes as perturbations of fundamental implicit difference schemes such as the backward-difference or Crank–Nicolson schemes.

For the present, it will be assumed that $\mathscr{D}(\phi)$ contains derivatives of first and second order with respect to $x$, $y$, and $z$, but no mixed derivatives. In this case, $\mathscr{D}$ can be split into three operators, $\mathscr{D}_x$, $\mathscr{D}_y$, $\mathscr{D}_z$ associated with the $x$, $y$, and $z$ coordinates and each having the functional form $\mathscr{D}_{\tilde{x}} = \mathscr{F}(\phi, \partial/\partial\tilde{x}, \partial^2/\partial\tilde{x}^2)$ for a typical coordinate $\tilde{x}$. Equation (16a) then becomes

$$[A + \Delta t(\mathscr{L}_x + \mathscr{L}_y + \mathscr{L}_z)]\,\psi^{n+1} = \Delta t[(\mathscr{D}_x + \mathscr{D}_y + \mathscr{D}_z)\,\phi^n + S^n]. \tag{17}$$

Recalling that $\mathscr{L}(\psi^n) = 0$, the Douglas–Gunn representation of (17)-can be written as the three-step solution procedure

$$(A + \Delta t\,\mathscr{L}_x)\,\psi^* = \Delta t[(\mathscr{D}_x + \mathscr{D}_y + \mathscr{D}_z)\,\phi^n + S^n], \tag{18a}$$

$$(A + \Delta t\,\mathscr{L}_y)\,\psi^{**} = A\psi^*, \tag{18b}$$

$$(A + \Delta t\,\mathscr{L}_z)\,\psi^{n+1} = A\psi^{**}, \tag{18c}$$

where $\psi^*$ and $\psi^{**}$ are intermediate solutions. It will be shown subsequently that each of (18) can be written in narrow block-banded matrix form and solved by efficient block-elimination methods. If $\psi^*$ and $\psi^{**}$ are eliminated, (18) becomes

$$\begin{aligned}(A + \Delta t\,\mathscr{L}_x)\,A^{-1}(A + \Delta t\,\mathscr{L}_y)\,A^{-1}(A + \Delta t\,\mathscr{L}_z)\,\psi^{n+1} \\ = \Delta t[(\mathscr{D}_x + \mathscr{D}_y + \mathscr{D}_z)\,\phi^n + S^n].\end{aligned} \tag{19}$$

If the multiplication on the left-hand side of (19) is performed, it becomes apparent that (19) approximates (17) to order $(\Delta t)^2$.

A major attraction of the Douglas–Gunn scheme is that the intermediate solutions $\psi^*$ and $\psi^{**}$ are consistent approximations to $\psi^{n+1}$. Furthermore, for steady solutions,

$\psi^n = \psi^* = \psi^{**} = \psi^{n+1} = 0$ independent of $\Delta t$. Thus, physical boundary conditions for $\psi^{n+1}$ can be used in the intermediate steps without a serious loss in accuracy and with no loss for steady solutions. In this respect, the Douglas–Gunn scheme appears to have an advantage over locally one-dimensional (LOD) or "splitting" schemes, and other schemes whose intermediate steps do not satisfy the consistency condition. The lack of consistency in the intermediate steps complicates the treatment of boundary conditions and, according to Yanenko [19, p. 33] does not permit the use of asymptotically large time steps. It is not clear that this advantage of the Douglas–Gunn scheme would always outweigh other benefits which might be derived from an alternative scheme. However, since the ADI scheme can be viewed as an approximate technique for solving the fundamental difference scheme (16a), alternate ADI schemes can readily be used within the present formulation.

It is worth noting that the operator $\mathscr{D}$ can be split into any number of components which need not be associated with a particular coordinate direction. As pointed out by Douglas and Gunn [1], the criterion for identifying suboperators is that the associated matrices be "easily solved" (i.e., narrow banded). Thus, mixed derivatives can be treated implicitly within the ADI framework, although this would increase the number of intermediate steps and thereby complicate the solution procedure. Finally, only minor complications result if $H$, $\mathscr{D}$, and $S$ are functions of the spatial coordinates and time, as well as $\phi$.

## Solution of the Implicit Difference Equations

### *Second-Order Spatial Differences*

Since each of (18) is implicit in only one coordinate direction, the solution procedure can be discussed with reference to a one-dimensional problem. For simplicity, it is sufficient to consider (18a) with $\mathscr{D}_y$, $\mathscr{D}_z = 0$. For the moment, attention is focused on the three-point difference formulas

$$D_{\tilde{x}}\phi \equiv [\alpha\Delta_- + (1-\alpha)\,\Delta_+]\phi/\Delta\tilde{x} = (\partial\phi/\partial\tilde{x})_i + O[\Delta\tilde{x}^2 + (\alpha - \tfrac{1}{2})\,\Delta\tilde{x}] \quad (20a)$$

$$D_{\tilde{x}}^2\phi \equiv (\Delta_+\Delta_-)\phi/(\Delta\tilde{x})^2 = (\partial^2\phi/\partial\tilde{x}^2)_i + O(\Delta\tilde{x}^2), \quad (20b)$$

for a typical coordinate $\tilde{x}$. Here, $\Delta_-\phi \equiv \phi_i - \phi_{i-1}$, $\Delta_+\phi \equiv \phi_{i+1} - \phi_i$, and a parameter $\alpha$ has been introduced ($0 \leqslant \alpha \leqslant 1$) so as to permit continuous variation from backward to forward differences. The standard central difference formula is recovered for $\alpha = \frac{1}{2}$ and was used for all solutions reported here.

As an example, suppose that the $q$th component of $\mathscr{D}_x$ has the form

$$\mathscr{D}_{xq}(\phi) = F_{1q}^T(\phi)\frac{\partial}{\partial x}G_{1q}(\phi) + F_{2q}^T(\phi)\frac{\partial^2}{\partial x^2}G_{2q}(\phi) \quad (21)$$

where $F$ and $G$ are column vector functions having the same but an arbitrary number

of components; $F^T$ denotes the transpose of $F$. The form of (21) permits governing equations having any number of first and second derivative terms. Then,

$$\Delta t \frac{\partial \mathscr{D}_{xq}}{\partial t} \simeq \frac{\partial \mathscr{D}_{xq}}{\partial \phi}(\phi^{n+1} - \phi^n) \equiv \left[F_{1q}^T \frac{\partial}{\partial x}\frac{\partial G_{1q}}{\partial \phi} + \frac{\partial G_{1q}^T}{\partial x}\frac{\partial F_{1q}}{\partial \phi}\right]^n (\phi^{n+1} - \phi^n)$$

$$+ \left[F_{2q}^T \frac{\partial^2}{\partial x^2}\frac{\partial G_{2q}}{\partial \phi} + \frac{\partial^2 G_{2q}^T}{\partial x^2}\frac{\partial F_{2q}}{\partial \phi}\right]^n (\phi^{n+1} - \phi^n). \tag{22}$$

It is now possible to describe the solution procedure for (18a) for the one-dimensional case with $\mathscr{D}_x$ given by (21) and difference formulas given by (20). Because of the spatial difference operators, $D_x$ and $D_x{}^2$, (18a) contains $\psi_{i-1}^*$, $\psi_i{}^*$, and $\psi_{i+1}^*$; consequently, the system of linear equations generated by writing (18a) at successive grid points $x_i$ can be written in block-tridiagonal form (simple tridiagonal for scalar equations, $l = 1$). The block-tridiagonal matrix structure emerges from rewriting (18a) as

$$a_i{}^n \psi_{i-1}^* + b_i{}^n \psi_i{}^* + c_i{}^n \psi_{i+1}^* = d_i{}^n \tag{23}$$

were $a$, $b$, $c$ are square matrices and $d$ is a column vector, each containing only $n$-level quantities. The $q$th component of $d$ and $q$th row-components of $a$, $b$, $c$ are given by

$$(a_i{}^n)_q = [(F_{1q}^T)_i(\partial G_{1q}/\partial\phi)_{i-1} + (G_{1q}^T)_{i-1}(\partial F_{1q}/\partial\phi)_i]^n \alpha/\Delta x$$

$$- [(F_{2q}^T)_i(\partial G_{2q}/\partial\phi)_{i-1} + (G_{2q}^T)_{i-1}(\partial F_{2q}/\partial\phi)_i]^n/(\Delta x)^2, \tag{24a}$$

$$(b_i{}^n)_q = (\partial H_q/\partial\phi)_i^n/\beta\,\Delta t - (\partial S_q/\partial\phi)_i^n$$

$$+ [(F_{1q}^T)_i(\partial G_{1q}/\partial\phi)_i + (G_{1q}^T)_i(\partial F_{1q}/\partial\phi)_i]^n(1 - 2\alpha)/\Delta x$$

$$+ 2[(F_{2q}^T)_i(\partial G_{2q}/\partial\phi)_i + (G_{2q}^T)_i(\partial F_{2q}/\partial\phi)_i]^n/(\Delta x)^2, \tag{24b}$$

$$(c_i{}^n)_q = [(F_{1q}^T)_i(\partial G_{1q}/\partial\phi)_{i+1} + (G_{1q}^T)_{i+1}(\partial F_{1q}/\partial\phi)_i]^n(\alpha - 1)/\Delta x$$

$$- [(F_{2q}^T)_i(\partial G_{2q}/\partial\phi)_{i+1} + (G_{2q}^T)_{i+1}(\partial F_{2q}/\partial\phi)_i]^n/(\Delta x)^2, \tag{24c}$$

$$(d_i{}^n)_q = [\mathscr{D}(\phi^n) + S^n]/\beta. \tag{24d}$$

When applied at successive grid points, (23) generates a block-tridiagonal system of equations for $\psi^*$ which, after appropriate treatment of boundary conditions, can be solved efficiently using standard block-elimination methods as discussed by Isaacson and Keller [20, p. 58]. The solution procedure for (18b) and (18c) is analogous to that just described for (18a). It is worth noting that the spatial difference parameter $\alpha$ can be varied with $i$ or even term by term. For example, an "upwind difference" formula can be obtained if $\alpha$ is chosen as 1 or $-1$ depending on the sign of the elements of $F_1$.

*Fourth-Order Spatial Differences*

Fourth-order spatial accuracy can be obtained by using the standard five-point difference formulas in place of (20)

$$D_{\tilde{x}}\phi = (1/2\Delta\tilde{x})(1 - \tfrac{1}{6}\Delta_+\Delta_-)(\Delta_+ + \Delta_-)\phi = (\partial\phi/\partial\tilde{x})_i + O(\Delta\tilde{x}^4), \tag{25a}$$

$$D_{\tilde{x}}{}^2\phi = (1/(\Delta\tilde{x})^2)(1 - \tfrac{1}{12}\Delta_+\Delta_-)(\Delta_+\Delta_-)\phi = (\partial^2\phi/\partial\tilde{x}^2)_i + O(\Delta\tilde{x}^4). \tag{25b}$$

In this instance, the block-tridiagonal structure of (23) expands to block pentadiagonal. Block-pentadiagonal systems are easily solved using banded Gaussian block elimination. Recently, there has been revived interest (e.g., Orszag and Israeli [21]) in the following fourth-order compact difference formulas involving only three grid points

$$D_{\tilde{x}}\phi = \frac{1}{2\Delta\tilde{x}} \frac{(\Delta_+ + \Delta_-)}{(1 + \frac{1}{6}\Delta_+\Delta_-)}\phi = (\partial\phi/\partial\tilde{x})_i + O(\Delta\tilde{x}^4), \tag{26a}$$

$$D_{\tilde{x}}{}^2\phi = \frac{1}{(\Delta\tilde{x})^2} \frac{(\Delta_+\Delta_-)}{(1 + \frac{1}{12}\Delta_+\Delta_-)}\phi = (\partial^2\phi/\partial\tilde{x}^2)_i + O(\Delta\tilde{x}^4). \tag{26b}$$

To implement (26) within the ADI framework, the difference equations are multiplied by the denominator of (26a) or (26b) at the appropriate step in the solution procedure (cf. [10], [11]).

## Computing Requirements

block-banded matrix structures (cf. [20]). Such algorithms can be derived using variants of Gaussian elimination for a banded matrix, but with the square submatrix elements of the banded matrix processed using matrix algebra. Thus, operations involving matrix subelements are not assumed to commute, and division by a matrix subelement is accomplished by computing the inverse and multiplying. Following this procedure, the authors have developed algorithms for both block-tridiagonal and block-pentadiagonal systems arising from the respective second- and fourth-order difference formulas, (20) and (25). Each algorithm requires only one inverse per grid point. A standard operation count (scalar multiplications and divisions) has been performed for systems with $L \times L$ block elements and $N$ diagonal block elements, i.e., $L$ coupled equations along $N$ grid points. The block-tridiagonal scheme requires $(3N - 2)(L^3 + L^2)$ operations, the same as the matrix factorization scheme of Isaacson and Keller [20]; the block-pentadiagonal scheme requires $(7N - 10)\,L^3 + (5N - 6)\,L^2$ operations, which is only slightly more than twice the block-tridiagonal number. Assuming there are $N$ grid points in each coordinate direction, the total number of operations for a single time step is obtained from the operation count for solution of one block-banded system by multiplying by $2N$ and $3N^2$ for two and three dimensions, respectively.

Based on computed results for a model problem, Orszag and Israeli [21, p. 284] have estimated that fourth-order schemes can achieve results in the 5% accuracy range with approximately half the number of grid points in each direction, as compared with second-order schemes. If this rough estimate is valid, it follows from the foregoing operation counts that for one-dimensional problems, use of the fourth-order scheme is roughly equivalent in terms of accuracy and computational cost to using the second-order scheme with twice as many grid points. In two and three dimensions, however, the second-order scheme would require four and eight times as many grid points, respectively, to obtain accuracy comparable to fourth-order schemes, and thus the fourth-order scheme would be worth the factor of two in computational effort per grid point.

For the particular case of the Navier–Stokes Eq. (3) with $p$ eliminated using (6), it is possible to reduce the computational effort substantially by taking advantage of the special nature of the coupling during each ADI sweep. In this case, it is only necessary to solve one block-banded system with $L = 3$, as well as two simple banded systems ($L = 1$). This can be seen by careful examination of (3). During the first step of the ADI procedure, only derivatives with respect to $x$ and $t$ from (3) appear in the implicit difference equations. In the continuity, $x$ momentum, and energy equations, these implicitly treated terms contain $\rho$, $u$, and $T$, but not $v$ and $w$; therefore, the difference equations from these three equations can be solved for $\rho^*$, $u^*$, and $T^*$ during the first ADI step by solving a block-banded system with $L = 3$. Having obtained values for $\rho^*$, $u^*$, and $T^*$ in this manner, the difference equations for the $y$ and $z$ momentum equations can then be solved independently for $v^*$ and $w^*$; since the $y$ and $z$ momentum equations are uncoupled with respect to $v^*$ and $w^*$ during this ADI step, the latter computation only requires the solution of two simple banded systems ($L = 1$). A similar situation exists for the remaining two steps of the ADI procedure, except that during the second step ( $y$ derivatives treated implicitly), the difference equations from the continuity, $y$ momentum, and energy equations are solved as coupled equations for $\rho^{**}$, $v^{**}$, and $T^{**}$, and during the third step ($z$ derivatives treated implicitly), the difference equations from the continuity, $z$ momentum, and energy equations are solved as coupled equations for $\rho^{n+1}$, $w^{n+1}$, and $T^{n+1}$.

For tridiagonal systems, the operation count is reduced from order 450 $N$ for one $L = 5$ system to order 118 $N$ for one $L = 3$ and two $L = 1$ systems. For pentadiagonal systems, these estimates are 1000 $N$ and 258 $N$, respectively. Consequently, the arrangement leading to three coupled and two uncoupled equations is quite worthwhile. For comparison, it is noted that in the case of the Navier–Stokes Eq. (3), merely evaluating the right-hand side of (18a), which would be a minimum requirement for a one-step explicit scheme, requires 302 $N$ operations for a three-point difference formula and 488 $N$ operations for a five-point formula.

In view of the many factors involved, it is difficult to evaluate precisely or with any generality the overall computational efficiency of the present method relative to various other methods. However, the foregoing operational counts show that the effort expended to solve the implicit difference equations by block elimination is

not excessive compared with that necessary simply to evaluate the differenced Navier–Stokes equations, let alone the various other bookkeeping tasks present in most large-scale computer programs for fluid dynamics problems. In the solutions presented here, the solution of the tridiagonal and block-tridiagonal systems using double precision arithmetic required only about one third to one half of the total computer time per time step.

## Application to Flow in a Straight Duct

### *Problem Formulation and Boundary Conditions*

To explore the stability properties and general capabilities of the present method, some test calculations were made for three-dimensional laminar subsonic flow in the entrance region of a straight duct with rectangular cross section. The flow geometry and coordinate system are shown in Fig. 1. The flow structure consists of boundary

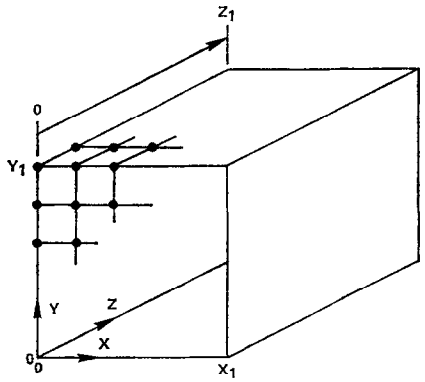


Fig. 1. Duct geometry and coordinate system.

layers on the duct walls and an inviscid core flow which accelerates due to the blockage effect of the boundary layers. At some downstream distance determined by the Reynolds number, the boundary layers grow to fill the duct and the flow becomes fully viscous. At this point, incompressible flows are fully developed or independent of axial distance. Compressible flows, however, undergo continuous acceleration due to frictional effects until at some axial distance the mean Mach number is unity and the flow becomes choked. Depending on the inlet Mach and Reynolds number, the flow may become choked either before or after it becomes fully viscous. For the present calculations, the duct length is chosen so that the flow at the exit is neither choked nor fully viscous.

Application of the present method is straightforward once $H$, $S$, and $\mathscr{D}$ are identified, and for the present calculations, these quantities are given in the Appendix. In applying the numerical method, the dissipation term, $\Phi$, defined by (5), and the

viscous terms in (4) containing $\nabla \cdot U$ were treated explicitly by evaluation at the $n$ level. This is accomplished by setting $\beta = 0$ in (16b). Although $\Phi$ could be treated implicitly and linearized, this would unnecessarily complicate the difference equations. The viscous terms involving $\nabla \cdot U$ contain mixed derivatives whose treatment by ADI methods is somewhat awkward, as mentioned previously. For the solutions presented here and other test cases computed while developing the method, the explicit treatment of the aforementioned viscous and dissipation terms had no observable adverse affect on stability. All solutions presented here were made using three-point centered difference formulas (i.e., $\alpha = \frac{1}{2}$ in (20)), and since steady solutions were the primary objective, the backward time difference form ($\beta = 1$) was employed throughout. In each case, the reference length, $L_r$, was taken as the duct width, and values of 0.73 and 1.4 were used for Pr and $\gamma$, respectively.

Boundary and initial conditions are required to complete the problem formulation. It is assumed that the duct is fed from a large stagnant reservoir. It is reasonable to assume that the flow upstream of the inlet plane is inviscid and adiabatic, and thus constant stagnation temperature $T_0$ and pressure $P_0$ are specified at the inlet plane. These quantities can be written in nondimensional form as

$$T_0 = T + ((\gamma - 1)/2)\, M^2 w^2 \tag{27a}$$

$$P_0 = (1/\gamma M^2)\, \rho T (T/T_0)^{\gamma/(1-\gamma)}. \tag{27b}$$

The $u$ and $v$ velocity components are small and were neglected in the definition of $T_0$. Including the $u$ and $v$ components in the definition of $T_0$ would couple all five governing equations at the upstream boundary during the $z$-direction step of the ADI procedure. Unless $u$ and $v$ were treated explicitly, this coupling would preclude, during this ADI step, the use of the more efficient solution technique previously described, in which only three equations are coupled. Implicit boundary conditions are obtained by writing (27) at the $(n + 1)$ level and linearizing by the same procedure employed for the governing equations at interior points. The velocity field at the inlet plane depends on conditions surrounding the inlet, and thus velocity boundary conditions must be modeled. The relation $D_z^2 w^{n+1} = 0$ was used at points adjacent to the upstream boundary. This boundary condition is equivalent to a linear extrapolation of $w^{n+1}$ on the upstream boundary from values at the two adjacent interior points (on a line in the $z$ direction), and will be referred to subsequently as implicit linear extrapolation. This boundary condition is compatible with the velocity behavior observed experimentally both in the boundary layers and inviscid core region. As the remaining upstream boundary conditions, the normal derivatives of $u^{n+1}$ and $v^{n+1}$ are set equal to zero using three-point, second-order, one-sided difference approximations. This is somewhat arbitrary, but reasonable.

At the downstream boundary, implicit linear extrapolation relations were used for $T^{n+1}$, $u^{n+1}$, $v^{n+1}$, and $w^{n+1}$, and the static pressure $P_s$, defined by

$$P_s = (1/\gamma M^2)\, \rho T \tag{27c}$$

is assumed constant. These conditions are once again reasonable if the duct is regarded as a portion of a longer duct, and also for a duct with an unobstructed exit into a large constant-pressure reservoir. The specified downstream static pressure, $P_s$, was an estimate of that required to maintain an average nondimensional velocity of 1.0 at the duct entrance.

No-slip conditions were specified on the walls of the duct, and adiabatic conditions were imposed by setting normal derivatives of temperature to zero using three-point, one-sided difference formulas. In addition, the wall density was determined implicitly using a three-point, one-sided difference approximation of the continuity equation. Since the flow is symmetric about the horizontal and vertical planes passing through the duct centerline, solutions were computed for one quadrant of the duct, and symmetry conditions were imposed on these planes of symmetry.

## Stability Tests

Two sequences of solutions were computed for Re = 60 with a $6 \times 6 \times 6$ grid and using different time steps, to explore the stability properties of the method. To provide a frame of reference, stability numbers $N_{\mathrm{CFL}}$ and $N_\mu$ are defined as the ratio of the actual time step $\Delta t$ to the maximum allowable time step as determined by the CFL and viscous stability limits, respectively, for one-dimensional uniform flow at the reference velocity and Mach number. These stability numbers are defined by

$$N_{\mathrm{CFL}} = (\Delta t/\Delta z)(1 + (1/M)), \tag{28a}$$

$$N_\mu = (2/\mathrm{Re})(\Delta t/(\Delta z)^2). \tag{28b}$$

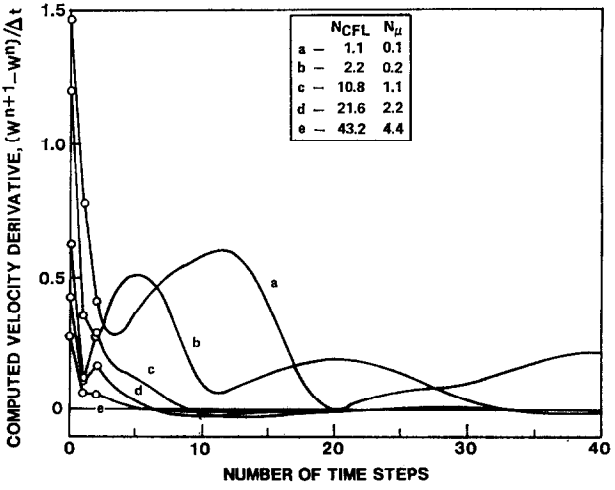


FIG. 2. Transient behavior of velocity time derivative at downstream centerline for different time steps; $M = 0.44$, Re = 60.

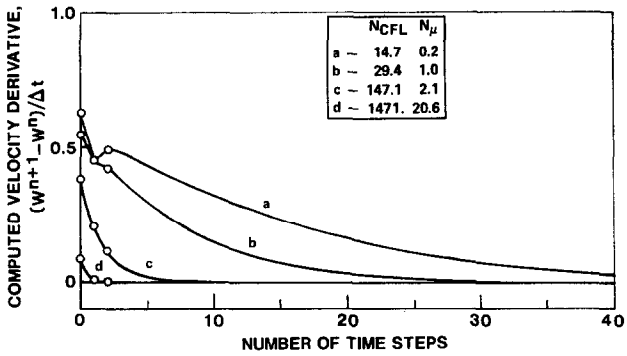


FIG. 3. Transient behavior of velocity time derivative at downstream centerline for different time steps; $M = 0.044$, Re $= 60$.

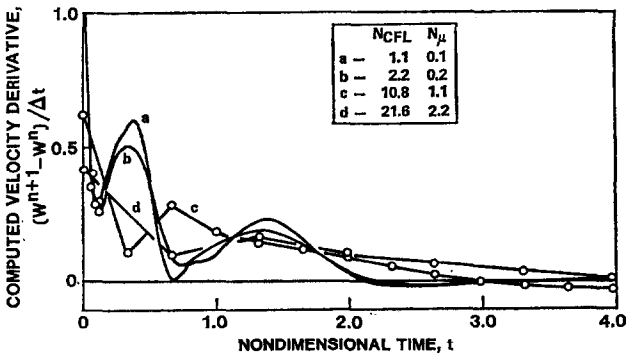


FIG. 4. Transient behavior of velocity time derivative at downstream centerline for different time steps; $M = 0.44$, Re $= 60$.

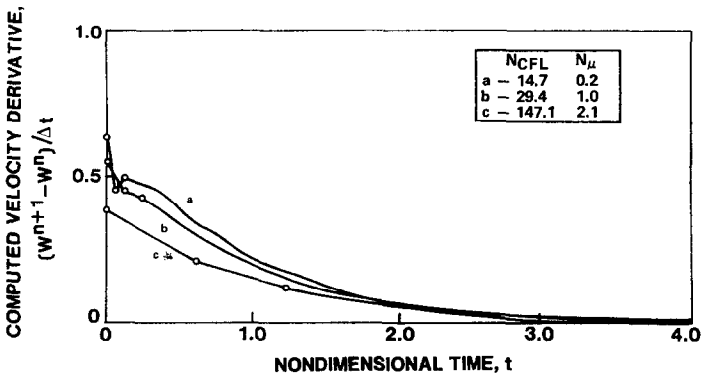


FIG. 5. Transient behavior of velocity time derivative at downstream centerline for different time steps; $M = 0.044$, Re $= 60$.

Typically, conditionally stable methods would require $N_{\mathrm{CFL}}$, $N_\mu \leqslant 1$ for stability. Multidimensional forms of (28) are more restrictive; however, splitting techniques can be employed (cf. [22]) to recover the one-dimensional forms. In actual computations with a conditionally stable method, the stability limits would vary from point to point with the local velocity, Mach number, and mesh size; however, (28) provides convenient reference quantities.

The initial conditions used for the stability tests are those appropriate for uniform flow in the $z$ direction at the reference velocity and with the specified stagnation pressure and temperature. At $t = 0$, the no-slip conditions were applied and the downstream static pressure was impulsively reduced to $P_s$. The duct geometry has $x_1 = y_1 = 1$, $z_1 = 0.5$.

The downstream centerline value of $(w^{n+1} - w^n)/\Delta t$ is a sensitive indicator of steady-state conditions and is shown in Fig. 2 for a sequence of solutions with $M = 0.44$. It can be seen that the method gave stable solutions for test cases in the range $N_{\mathrm{CFL}} \leqslant 43.2$, $N_\mu \leqslant 4.4$, and that steady conditions were reached with significantly fewer time steps for higher $N_{\mathrm{CFL}}$. A second sequence of solutions was computed for $M = 0.044$, and similar results were obtained (Fig. 3) for $N_{\mathrm{CFL}} \leqslant 1471$, $N_\mu \leqslant 20.6$.

The transient accuracy of the $M = 0.44$ test cases can be assessed in Fig. 4, although as mentioned earlier, transient accuracy was not an objective of these calculations. The solutions in Fig. 4 are not independent of the time step ($N_{\mathrm{CFL}}$), and thus there is temporal truncation error in these solutions. However, curves a and b display far less dependence on $N_{\mathrm{CFL}}$ than the remaining curves, and thus it appears that convergence is beginning for $N_{\mathrm{CFL}} \leqslant 2.2$. Steady-state conditions are reached in a nondimensional time on the order of four for curves a and b. Clearly, the temporal truncation error is much greater for curves c and d ($10.8 \leqslant N_{\mathrm{CFL}} \leqslant 21.6$), although these latter cases reached steady state in fewer time steps (Fig. 2). Similar plots of the transient solution

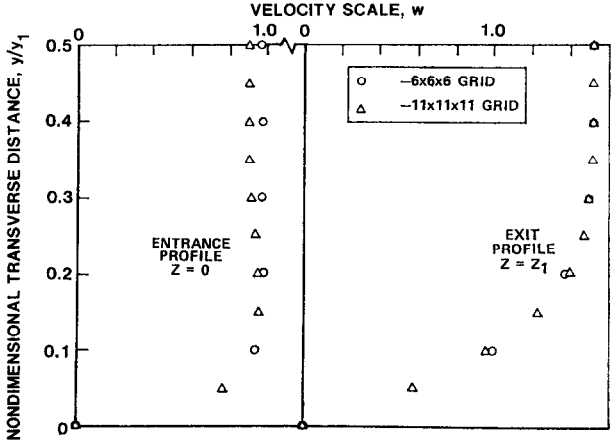


FIG. 6. Effect of mesh size on computed axial velocity profiles at $x/x_1 = 0.5$; $M = 0.44$, Re = 60.

for the $M = 0.044$ test cases are given in Fig. 5. It should be emphasized that the degree of transient accuracy indicated in Figs. 4 and 5 is not a *general* indication of the accuracy achievable at a given $N_{CFL}$ or $N_{\mu}$ with the present method, since these stability tests involve first-order backward time differences, a very coarse mesh, and impulsive starting conditions.

The effect of mesh size on computed solutions was examined empirically for the $M = 0.44$ test case. Axial velocity profiles are compared in Fig. 6 for two solutions having $6 \times 6 \times 6$ and $11 \times 11 \times 11$ grids in the computed quadrant of the duct; the two solutions are in satisfactory agreement. The error is larger at the duct entrance, where the inlet conditions are somewhat severe for the mesh spacing used. In Fig. 7, centerline velocity and pressure are shown for three solutions having 6, 11, and 21 mesh

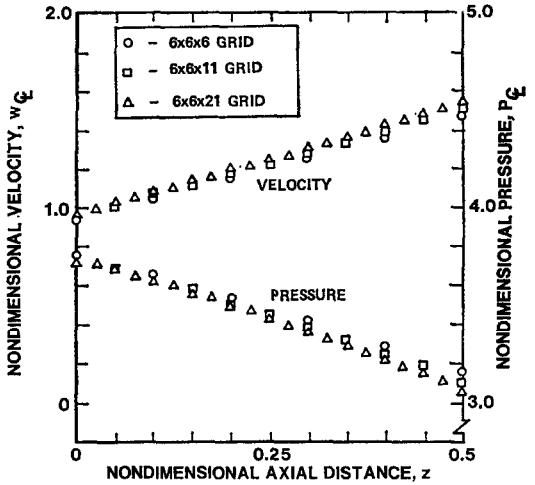


FIG. 7. Effect of axial mesh size on computed centerline velocity and pressure; $M = 0.44$, $\mathrm{Re} = 60$.

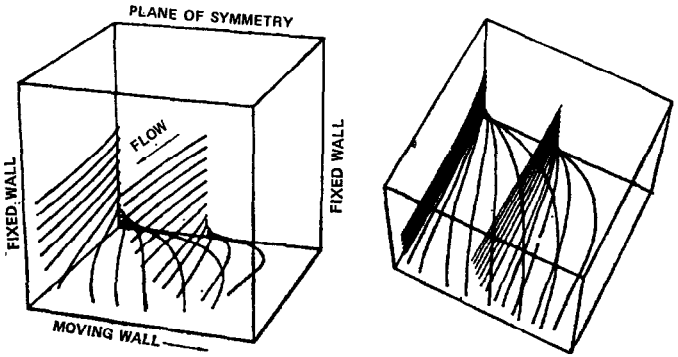


FIG. 8. Selected streamlines for duct flow With moving walls; $M = 0.44$, $\mathrm{Re} = 60$.

points in the $z$ direction. This comparison also reflects a reasonable influence of mesh size on the solutions.

An additional solution was computed for $M = 0.44$, $\mathrm{Re} = 60$ but with a large secondary flow caused by moving two parallel duct walls in a direction perpendicular to the axial flow direction; the wall speed is about 25% of the average axial velocity. Since the flow is symmetric about a horizontal plane midway between the moving walls only the lower half of the flow field was computed, and computer-produced drawings of selected streamlines for this solution are shown in Fig. 8. No data or other theoretical studies are available for comparison in this instance and the computed solutions are presented largely as a demonstration of stability in the presence of large secondary flows.

## High Reynolds Number Solutions

### *Nonuniform-Grid Transformation*

The accuracy of solutions computed with a given number of grid points can often be improved by using a nonuniform grid spacing to ensure that grid points are closely spaced in regions where the solution varies rapidly and widely spaced elsewhere. An analytical coordinate transformation has been devised by Roberts [23] which is an effective means of introducing a nonuniform grid when the steep gradients occur near the computational boundaries. If $N$ grid points are to be used in the range $0 \leqslant x \leqslant 1$, and if steep gradients are anticipated in a region of thickness $\sigma$ near $x = 0$, then Roberts' transformation $\eta(x)$ is given by

$$\eta(x) = N + (N - 1) \log \left( \frac{x + a - 1}{x + a + 1} \right) \Big/ \log \left( \frac{a + 1}{a - 1} \right) \tag{29}$$

where $a^2 = 1/(1 - \sigma)$. The use of equally-spaced points in the transformed coordinate $\eta$ provides resolution of both the overall region $0 \leqslant x \leqslant 1$ and the subregion $0 \leqslant x \leqslant \sigma$. Transformation (29) was employed in high Reynolds number solutions to provide increased resolution near the duct entrance and in boundary layers on the duct walls. Values of 0.1, 0.1, and 0.25 were used as $\sigma$ for the $x$, $y$, and $z$ coordinates, respectively.

### *Artificial Dissipation*

In computing solutions for high Re, it was necessary to add a form of artificial viscosity or dissipation for the axial flow direction. Artificial dissipation in some form is often useful in practical calculations to stabilize the overall method when boundary conditions are treated inaccurately, when coarse mesh spacing is used, or in the presence of discontinuities. (von Mises [24] has shown that certain discontinuities in solutions of the Navier–Stokes equations are possible despite the presence of physical viscosity and heat conduction terms.) The need for artificial dissipation arises in certain

instances when centered spatial difference approximations are used for first derivative terms. The use of artificial dissipation is thus a matter of spatial differencing technique, and is commonly employed in either explicit or inherent form and in both explicit and implicit difference schemes. The particular form described here was adequate for present purposes but is considered provisional and is not recommended for general use, since the formal accuracy is lowered to first order for the axial ($z$) coordinate direction.

The dissipation term used here is based on an observation (e.g., Roache [25, p. 162]) that for a linear model problem representing a one-dimensional balance of convection and diffusion terms, solutions obtained using central differences for the convection term are well behaved provided the mesh Reynolds number $\mathrm{Re}_{\Delta z} = | w | \Delta z \, \mathrm{Re}$ is $\leqslant 2$. but that qualitative inaccuracies (associated with boundary conditions) occur for $\mathrm{Re}_{\Delta z} > 2$. This suggests the use of an artificial viscosity term of the form $\epsilon_z D_z{}^2\phi$, where

$$\begin{aligned} \epsilon_z &= \frac{| w | \Delta z}{2} - \frac{1}{\mathrm{Re}} = \frac{1}{\mathrm{Re}}\left(\frac{\mathrm{Re}_{\Delta z}}{2} - 1\right), && \mathrm{Re}_{\Delta z} > 2, \\ &= 0, && \mathrm{Re}_{\Delta z} \leqslant 2, \end{aligned} \tag{30}$$

to ensure that the local effective mesh Reynolds number is no greater than two. This dissipation term was added to each of the governing equations, with $\phi$ taken as $\rho$ for the continuity equation, $u$, $v$, $w$ for the respective $x$, $y$, and $z$ momentum equations, and $T$ for the energy equation. For scalar equations, the foregoing technique is equivalent to that developed by Spalding [26] from an argument not involving artificial viscosity.

*Computed Solution*

A solution is presented for $M = 0.3$, $\mathrm{Re} = 600$, and a duct geometry for which $x_1 = y_1 = 1$, $z_1 = 5$. An $11 \times 11 \times 21$ grid was used, along with a variable time

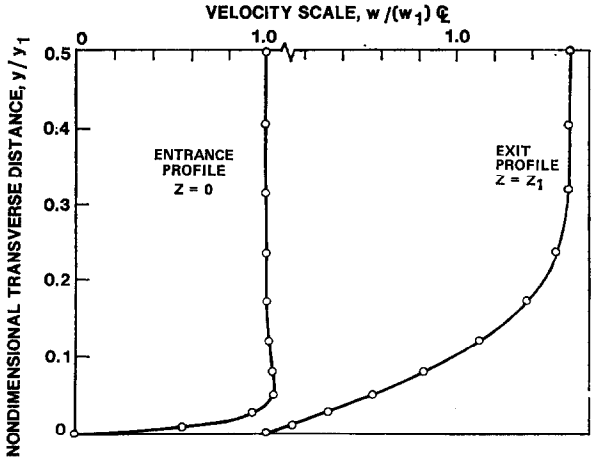


FIG. 9. Computed axial velocity profiles at $x/x_1 = 0.5$; $M = 0.3$, $\mathrm{Re} = 600$.

step with $N_{CFL}$ up to 380 and, $N_{\mu}$ up to 12. Computed axial velocity profiles at the duct entrance and exit are shown in Fig. 9 for this case. The subscript 1 denotes conditions at the duct entrance. The axial variation of pressure ratio and Mach number is given in Fig. 10. As a check on the solution, two additional pressure curves are shown. One curve represents the pressure ratio from one-dimensional theory for adiabatic, frictional, constant-area flow of a perfect gas [27]. Using this theory, the pressure ratio between two points can be evaluated if the Mach numbers are known; the

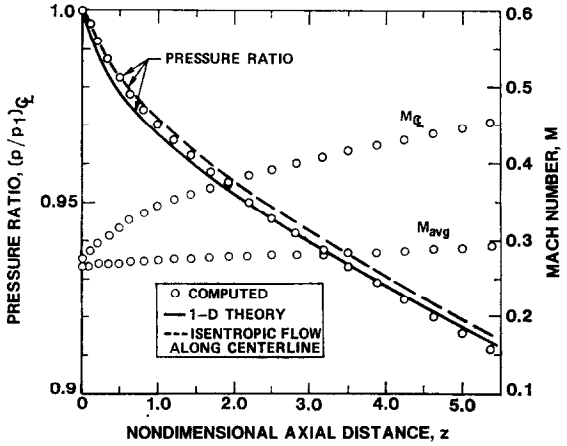


FIG. 10. Axial variation of pressure ratio and Mach number; $M = 0.3$, Re = 600.

average Mach number, $M_{avg}$ (averaged over the cross section) from the Navier–Stokes solution was used for this evaluation. The second curve assumes isentropic flow and constant stagnation pressure along the centerline of the duct and was evaluated from the isentropic relations for a perfect gas using the computed centerline Mach number, $M_{\Phi}$. The general agreement of pressure ratio distributions seen in Fig 10 is an indication of internal consistency in the computed solution. Since the average inlet Mach number is only 0.27, and since the axial variation in density is only about 8 %, compressibility effects should be relatively minor for this solution The computed pressure drop was therefore compared with the experimental measurements of Beavers *et al.* [28] for incompressible flow and found to be in reasonable agreement, considering the difference in $M$. The results of this comparison are shown in Fig. 11.

In assessing the high Reynolds number solution, the question arises as to whether the artificial viscosity destroys the accuracy by changing the effective Reynolds number of a viscous calculation. Here, it should be emphasized that the artificial viscosity was used only for the axial coordinate direction, where viscous terms are generally unimportant; second-order accuracy was rigorously maintained for the two transverse directions, for which viscous stresses are large The magnitude of the artificial viscosity terms in the computed solutions was examined a posteriori and compared with other terms in the equations. It was found that the artificial viscosity

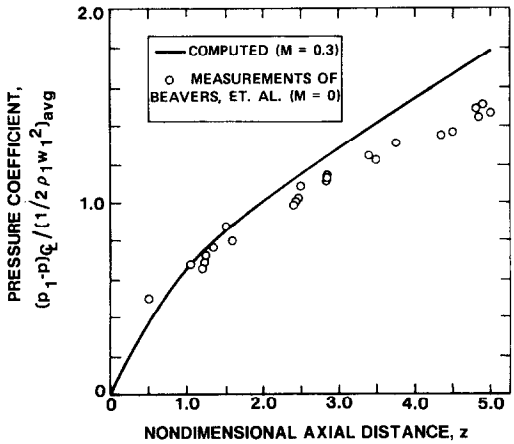


FIG. 11. Comparison of computed and measured axial pressure drop; $M = 0.3$, Re = 600.

terms were no greater than about 2% of the largest term in each equation, except at grid points very near the edges of the duct walls at the entrance The specification of constant stagnation pressure and temperature at the entrance along with the no-slip conditions on the walls produces very large gradients in this region, and the artificial viscosity terms were as large as 15 to 20% there. It is believed, however, that the accuracy was not seriously degraded by the artificial viscosity except, of course, locally near the entrance edges of the walls. As a final check on the solutions, the mass flow rate was computed by integration of $w$ over the cross section at each axial location in the duct and was found to be constant to within 0.4%.

The UNIVAC 1108 run time for the solutions presented here was about $3.5 \times 10^{-4}$ minutes per grid point per time step, which includes the use of auxiliary storage devices Solution of the implicit difference equations was performed in double precision. Convergence to a steady solution required from 20 to 100 time steps, depending on how the time step was chosen.

## APPENDIX

Terms in governing equation (3) are arranged for application of the numerical method as

$$H^T = (\rho, \rho u, \rho v, \rho w, \rho T), \tag{A1}$$

$$\mathscr{D}_x(\phi) = \begin{pmatrix} -\partial(\rho u)/\partial x \\ -\partial(\rho u^2 + \rho T/\gamma M^2)/\partial x + \partial^2(u/\mathrm{Re})/\partial x^2 \\ -\partial(\rho uv)/\partial x + \partial^2(v/\mathrm{Re})/\partial x^2 \\ -\partial(\rho uw)/\partial x + \partial^2(w/\mathrm{Re})/\partial x^2 \\ -\partial(\rho uT)/\partial x + (1-\gamma)\,\rho T\,\partial u/\partial x + \partial^2(\gamma T/\mathrm{Re\,Pr})/\partial x^2, \end{pmatrix} \tag{A2}$$

$$\mathscr{D}_y(\phi) = \begin{pmatrix} -\partial(\rho v)/\partial y \\ -\partial(\rho uv)/\partial y + \partial^2(u/\mathrm{Re})/\partial y^2 \\ -\partial(\rho v^2 + \rho T/\gamma M^2)/\partial y + \partial^2(v/\mathrm{Re})/\partial y^2 \\ -\partial(\rho vw)/\partial y + \partial^2(w/\mathrm{Re})/\partial y^2 \\ -\partial(\rho vT)/\partial y + (1-\gamma)\,\rho T\,\partial v/\partial y + \partial^2(\gamma T/\mathrm{Re\,Pr})/\partial y^2, \end{pmatrix} \tag{A3}$$

$$\mathscr{D}_z(\phi) = \begin{pmatrix} -\partial(\rho w)/\partial z \\ -\partial(\rho uw)/\partial z + \partial^2(u/\mathrm{Re})/\partial z^2 \\ -\partial(\rho vw)/\partial z + \partial^2(v/\mathrm{Re})/\partial z^2 \\ -\partial(\rho w^2 + \rho T/\gamma M^2)/\partial z + \partial^2(w/\mathrm{Re})/\partial z^2 \\ -\partial(\rho wT)/\partial z + (1-\gamma)\,\rho T\,\partial w/\partial z + \partial^2(\gamma T/\mathrm{Re\,Pr})/\partial z^2, \end{pmatrix} \tag{A4}$$

$$S^T = \left(0, \frac{1}{3\,\mathrm{Re}}\frac{\partial(\nabla\cdot U)}{\partial x}, \frac{1}{3\,\mathrm{Re}}\frac{\partial(\nabla\cdot U)}{\partial y}, \frac{1}{3\,\mathrm{Re}}\frac{\partial(\nabla\cdot U)}{\partial z}, \gamma(\gamma-1)\,M^2\Phi/\mathrm{Re}\right). \tag{A5}$$

## Acknowledgment

This work was supported by the Office of Naval Research under Contract N00014-72-C-0183. During the preparation of the manuscript, the authors have benefited from several discussions with Dr. Peter R. Eiseman.

## References

1. J. Douglas and J. E. Gunn, *Numer. Math.* **6** (1964).
2. A. J. Chorin, A numerical method for solving incompressible viscous flow problems, *J. Computational Phys.* **2** (1967), 12.
3. C. E. Pearson, *J. Fluid Mech.* **21** (1965), 611.
4. A. J. Chorin, *Math. Comp.* **22** (1968), 745.
5. F. H. Harlow and A. A. Amsden, *J. Computational Phys.* **8** (1971), 197.
6. E. Baum and E. Ndefo, "Proceedings of the AIAA Computational Fluid Dynamics Conference, New York," p. 133, 1973.
7. D. W. Peaceman and H. H. Rachford, *J. Soc. Ind. Appl. Math.* **3** (1955), 28.
8. H. McDonald and W. R. Briley, *J. Computational Phys.* **19** (1975), 150.
9. W. R. Briley and H. McDonald, Solution of the three-dimensional compressible Navier–Stokes equations by an implicit technique, *in* "Proceedings of the Fourth International Conference on Numerical Methods in Fluid Dynamics," Springer–Verlag, New York, 1975. See also, United Aircraft Research Laboratories Report M911363-6 (1973).
10. R. M. Beam and R. F. Warming, *J. Computational Phys.* **22** (1976), 87.
11. A. R. Mitchell, "Computational Methods in Partial Differential Equations," Wiley, New York, 1969.
12. W. F. Ames, "Numerical Methods for Partial Differential Equations," Barnes & Noble, New York, 1969.
13. D. A. von Rosenberg, "Methods for the Numerical Solution of Partial Differential Equations," American Elsevier, New York, 1969.
14. J. Douglas and B. F. Jones, *J. Soc. Ind. Appl. Math.* **11** (1963), 195.

15. A. R. GOURLAY AND J. L. MORRIS, *Math. Comp.* **22** (1968), 28.
16. R. D. RICHTMYER AND K. W. MORTON, "Different Methods for Initial Value Problems," 2nd ed., Interscience, New York, 1967.
17. R. E. BELLMAN AND R. E. KALABA, "Quasilinearization and Nonlinear Boundary Value Problems," American Elsevier, New York, 1965.
18. J. DOUGLAS, *J. Soc. Ind. Appl. Math.* **3** (1955), 42.
19. N. N. YANENKO, "The Method of Fractional Steps," Springer–Verlag, New York, 1971.
20. E. ISAACSON AND H. B. KELLER, "Analysis of Numerical Methods," Wiley, New York, 1966.
21. S. A. ORSZAG AND M. ISRAELI, Numerical simulation of viscous incompressible flows, *in* "Annual Reviews in Fluid Mechanics," Vol. 6, p. 281, Annual Reviews, Inc., 1974.
22. R. W. MACCORMACK AND A. J. PAULLAY, AIAA Paper No. 72-154 (1972).
23. G. O. ROBERTS, Computational meshes for boundary layer problems, *in* "Proceedings of the 2nd International Conference on Numerical Methods in Fluid Dynamics," p. 171, Springer–Verlag, New York, 1971.
24. R. VON MISES, On some topics in the fundamentals of fluid flow theory, *in* "Proceedings of the 1st U. S. National Congress of Applied Mechanics," p. 667, ASME, 1951.
25. P. J. ROACHE, "Computational Fluid Dynamics," Hermosa, Albuquerque, New Mexico, 1972.
26. D. B. SPALDING, *Int. J. Num. Meth. Eng.* **4** (1972), 551.
27. A. S. SHAPIRO, "The Dynamics and Thermodynamics of Compressible Fluid Flow," Vol. I, p. 162, Ronald Press, New York, 1953.
28. G. S. BEAVERS, E. M. SPARROW, AND R. A. MAGNUSON, *Int. J. Heat Mass Transfer* **13** (1970), 689.